Product Datasheet

Histone H2AX [p Ser139] Antibody
NB100-384

Unit Size: 0.1 ml

Store at 4C. Do not freeze.

www.novusbio.com technical@novusbio.com

Reviews: 1 Publications: 156

Protocols, Publications, Related Products, Reviews, Research Tools and Images at:
www.novusbio.com/NB100-384

Updated 12/20/2023 v.20.1

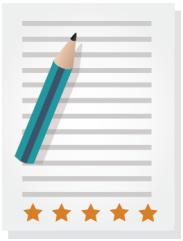

NB100-384

Histone H2AX [p Ser139] Antibody

Product Information	
Unit Size	0.1 ml
Concentration	1.0 mg/ml
Storage	Store at 4C. Do not freeze.
Clonality	Polyclonal
Preservative	0.09% Sodium Azide
Isotype	IgG
Purity	Immunogen affinity purified
Buffer	Tris-Citrate/Phosphate (pH 7.0 - 8.0)
Target Molecular Weight	15 kDa

Product Description	
Host	Rabbit
Gene ID	3014
Gene Symbol	H2AX
Species	Human, Mouse, Rat, Canine
Reactivity Notes	Rat reactivity reported in scientific literature (PMID: 27102221), Canine reactivity reported in scientific literature (PMID: 23365434).
Marker	DNA Double-strand break marker
Specificity/Sensitivity	The epitope maps to a region surrounding phosphorylated serine 139 of human histone H2AX.
Immunogen	This Histone H2AX [p Ser139] Antibody was developed against to a region surrounding phosphorylated serine 139 of human histone H2AX [Swiss-Prot entry P16104] (GeneID 3014).
Notes	Licensed to Novus Biologicals LLC under U.S. Patent Nos. 6,362,317 and 6,884,873.

Product Application Details	
Applications	Western Blot, Simple Western, Flow Cytometry, Immunocytochemistry/ Immunofluorescence, Immunohistochemistry, Immunohistochemistry-Frozen, Immunohistochemistry-Paraffin, Chromatin Immunoprecipitation (ChIP), Knockout Validated
Recommended Dilutions	Western Blot 1:10000-1:25000, Simple Western 5 ug/ml, Flow Cytometry 5 ug per 1 million cells, Immunohistochemistry 1:2000 - 1:10000, Immunocytochemistry/ Immunofluorescence 1:500 to 1:5000, Immunohistochemistry-Paraffin 1:2000 - 1:10000, Immunohistochemistry-Frozen 1:1000 - 1:5000, Chromatin Immunoprecipitation (ChIP), Knockout Validated
Application Notes	For IHC, epitope retrieval with citrate buffer pH6.0 is recommended for FFPE tissue sections. Formaldehyde fixation is recommended. Permeabilization with Triton-X 100 is recommended for formaldehydefixed cells. Immunoprecipitation is not recommended. In Simple Western only 10 - 15 uL of the recommended dilution is used per data point. Separated by Size-Wes, Sally Sue/Peggy Sue. Use in chromatin immunoprecipitation reported in scientific literature (PMID: 30049290).

Images

Detection of Human and Mouse Histone H2AX [p Ser139] by Western Blot. Samples: Nuclear extract (50 ug) from human HEK293, human melanoma (G361), mouse wildtype embryonic fibroblasts (+/+) or mouse H2AX knockout embryonic fibroblasts (-/-). Antibody: Affinity purified rabbit Histone H2AX [p Ser139] antibody NB100-384 used at 0.1 ug/ml. Detection: Chemiluminescence with 30 second exposure. (NCS, neocarzinostatin - 200 ng/ml, 30 min). Bands appear at an observed molecular weight of ~15 kDa.	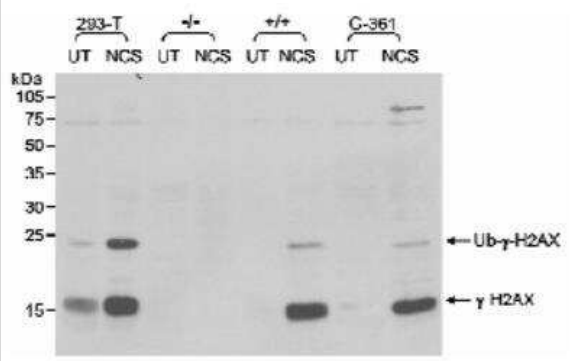
Samples: Neocarzinostatin treated asynchronous HeLa cells (left) and untreated asynchronous HeLa cells (right) . Antibody: Affinity purified rabbit Histone H2AX [p Ser139] used at a dilution of 1:5,000 (0.2ug/ml). Detection: Red fluorescent Anti-rabbit IgG-DyLight 594 used at a dilution of 1:100.	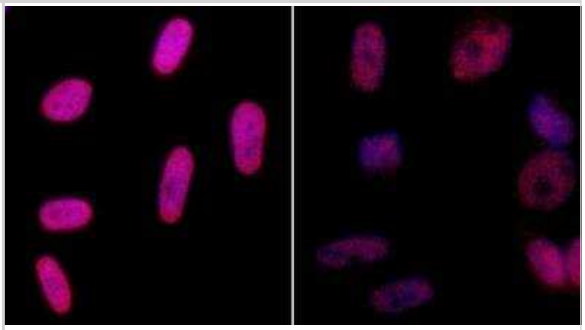
Simple Western lane view shows a specific band for Histone H2AX [p Ser139] in 0.2 mg/ml of Jurkat lysate(s). This experiment was performed under reducing conditions using the 12 - 230 kDa separation system.	
Immunocompromised mice were subcutaneously injected with cancerous cell lines and tumors were allowed to establish. Treatments occurred every other day and the studied compound or the equivalent vehicle control administered intraperitoneally for five weeks. Tumor volume and mass were measured two times per week. IHC analysis of sectioned tumor tissues from the MDA-MB-231 study. Each section was subjected to the specified antibody followed by a biotinylated secondary antibody. Detection was done using a DAB Peroxidase HRP Substrate Kit (brown) followed by Hematoxylin counterstaining (purple). Images were obtained using inverted bright field microscopy. Sectioning results are representative of three individual tumors. Scale bar is 50 microns. Image collected and cropped by CiteAb from the following publication (nature.com/articles/s41598-017-01230-4), licensed under a CC-BY license.	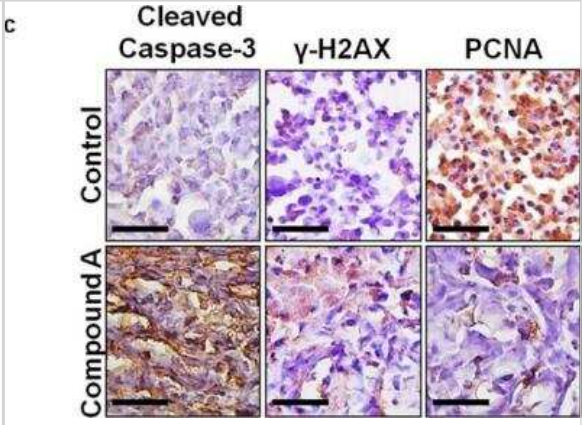

Immunostaining of Histone H2AX [p Ser139] WT1 and 5mC in patients with IgA nephropathy and controls. Examples of PAS staining and immunostaining with Histone H2AX [p Ser139] (green) and WT1 (red), pATM and 5mC in glomeruli of IgA nephropathy and controls. A kidney sample of a 65-year-old male of IgA nephropathy without podocytopathic features. Arrows indicate Histone H2AX [p Ser139] and WT1 double-positive cells. Scale bars: 50um. Image collected and cropped by CiteAb from the following publication (https://www.nature.com/articles/s41598-019-57140-0) licensed under a CC-BY license.	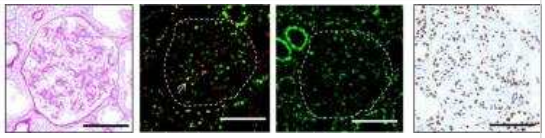
Samples: Nuclear extract from HeLa cells treated with 100 uM EPE for 4 hours (+) or mock treated (-). Antibody: Affinity purified rabbit Histone H2AX [p Ser139] antibody used at 0.1 ug/ml. Detection: Chemiluminescence with an exposure time of 3 minutes. Band appears at an observed molecular weight of ~17 kDa.	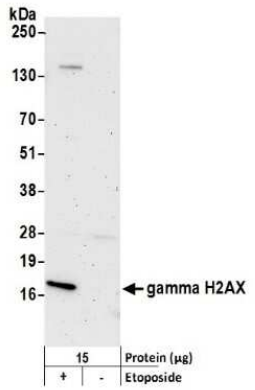
Detection of human Histone H2AX [p Ser139] by western blot. Samples: Whole cell lysate (50 ug) from Jurkat cells treated with 100 uM EPE for 4 hours (+) or mock treated (-). Antibody: Affinity purified rabbit Histone H2AX [p Ser139] antibody NB100-384 used for WB at 0.1 ug/ml. Detection: Chemiluminescence with an exposure time of 3 seconds. Band appears at an observed molecular weight of ~18 kDa.	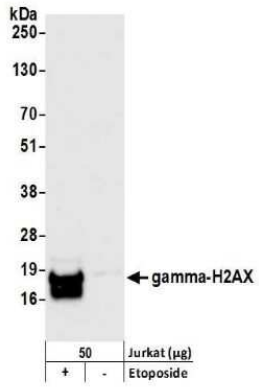
FFPE section of mouse CT26 colon carcinoma. Antibody: Affinity purified rabbi Histone H2AX [p Ser139] antibody used at a dilution of 1:1,000 (1 ug/ml). Detection: DAB.	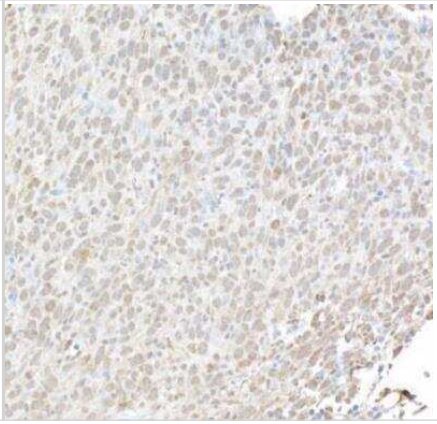

Analysis of Histone H2AX [p Ser139] in EPE Treated Jurkat Cells. Cells were treated for 3 hrs in 5ug/ml etoposide, fixed in 1.5% PFA, and permeabilized in 90% Methanol. 1 million cells were stained with 0.5 ug anti-KLH or anti-H2AX NB100-384 and secondary FITC-conjugated goat anti-rabbit (in a 150ul reaction). Black- etosposide treated, anti-KLH; Red- untreated, anti-Histone H2AX [p Ser139]; Blue- etoposide treated , anti-Histone H2AX [p Ser139].	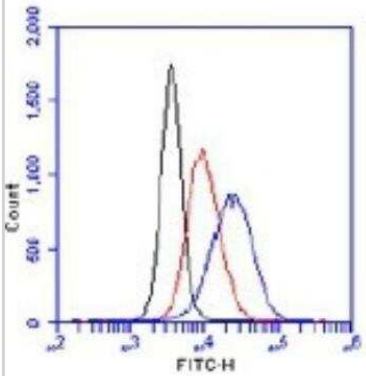
FFPE section of human ovarian carcinoma. Antibody: Affinity purified rabbit Histone H2AX [p Ser139] antibody used at a dilution of 1:5,000 (0.2 ug/ml). Detection: DAB.	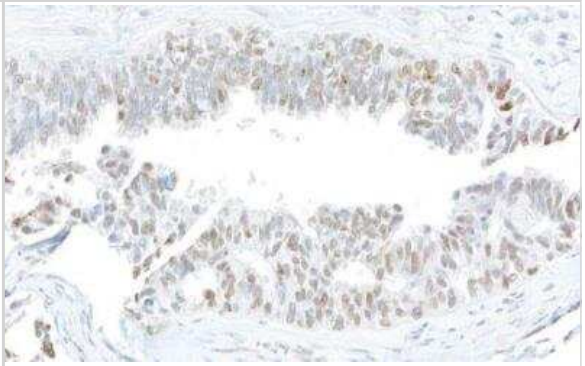
Electropherogram image(s) of corresponding Simple Western lane view. Histone H2AX [p Ser139] antibody was used at 5 ug/ml dilution on Jurkat lysate(s).	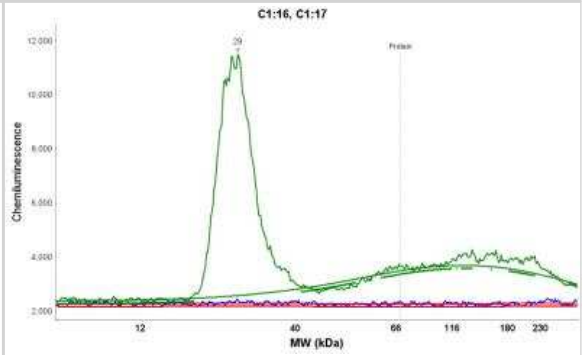
Immunohistochemistry: Rabbit Polyclonal Histone H2AX [p Ser139] Antibody - Histone H2AX Antibody on mouse cancer tissue. H2AX (Gray) and H2BGFP(Green). Primary antibody dilution: 1:1000 in a 10um slice.	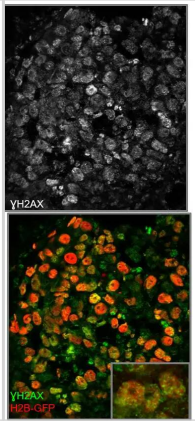

mTORC1/2 activity prevents Cisplatin-induced cell death in MCF-10A cells. (A) Western blot displaying effects on mTOR signaling during a dose escalation of PP242 treatment in MCF-10A cells; (B) Western blot displaying effects of mTOR signaling on a dose escalation of cisplatin treatment in MCF-10A cells; (C) Western blot displaying effects on mTOR signaling and cell death during non-treated, Cisplatin, PP242, and Cisplatin + PP242-treated MCF-10A cells.	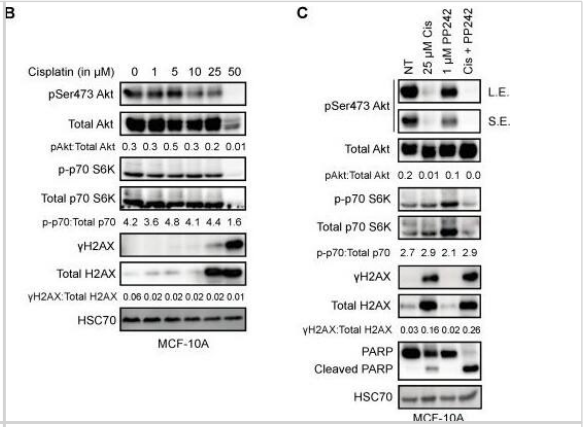
ERM expression and localization in SKBR3 breast cancer cells(A) Western blot analysis of ERM levels in SKBR3, HeLa and PC3 cells. SKBR3 breast cancer cells do not express moesin. (B) Colocalization of ezrin/radixin and ErbB2 in SKBR3 cells. 3D-SIM of fixed cells, stained for endogenous ERM and ErbB2, shows a high degree of colocalization between the ezrin/radixin and ErbB2 at the plasma membrane (left panel: max. projection; middle: single plane section; right: single channels of insert). Scale bars: 10 μm. (C) Analysis of protein association in SKBR3 cells by proximity ligation assay (PLA). 2 h treatment with 3 μM GA leads to decreased association of ezrin/ErbB2 and radixin/ErbB2. Data is represented as mean +/− SEM (***P < 0.001). (D) Corresponding single plan section of a representative PLA experiment. Fluorescence and DIC pictures of control cells (upper panel) and cell treated for 2 h with geldanamycin (lower panel) are shown. Scale bars: 10 μm. Image collected and cropped by CiteAb from the following open publication (https://pubmed.ncbi.nlm.nih.gov/27029001), licensed under a CC-BY license. Not internally tested by Novus Biologicals.	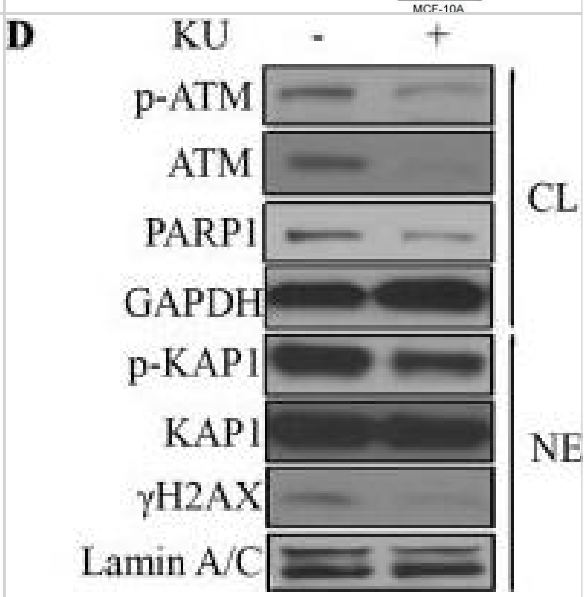
Digital image analysis of cytoplasmic and membranous staining. Cytoplasmic HIF-1α staining is shown (A) and automated image analysis utilizing TissueIA recognizes cytoplasmic HIF-1α staining highlighted in green color (B). CA9 is shown in membranous staining (C) and automated image analysis determines membranous CA9 staining highlighted in green color (D). The output from the algorithm returns a number of quantitative measurements for intensity and percentage of positive staining present. Scale bar: 100 μm. Image collected and cropped by CiteAb from the following open publication (https://translational-medicine.biomedcentral.com/articles/10.1186/1479-5876-11-185), licensed under a CC-BY license. Not internally tested by Novus Biologicals.	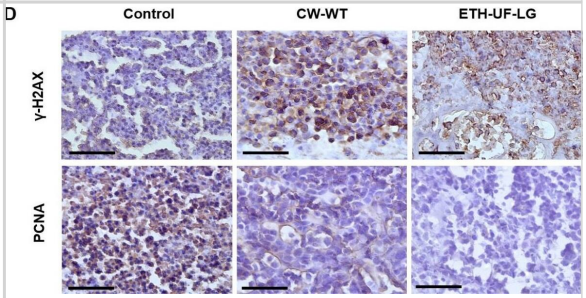

PHD3 elevates p27 expression through a post-translational mechanism. a PHD3 depletion has no effect on p27 transcription under hypoxia. p27 mRNA levels were measured in HeLa cells using quantitative real-time PCR. Results shown as fold change vs normoxic control, four independent experiments (± SEM) (p = n.s.; n = 4). b Hypoxic p27 expression is HIF-1α and EPAS1/HIF-2α independent. QRT-PCR analysis of p27 and hypoxia-inducible glut-1 mRNA normalized to β-actin using the indicated double knockdown after 24 h of hypoxia. Unlike glut-1 HIF knockdown has little effect on p27 transcription. Results from three independent experiments (±SEM) are shown (p = n.s.; n = 3). c PHD3 depletion induces p27 protein levels independently of HIF-1α or EPAS1/HIF-2α depletion in HeLa cells. d Quantification of p27 protein expression using indicated double knockdown. Results from three independent experiments (±SEM) are shown Image collected and cropped by CiteAb from the following open publication (https://pubmed.ncbi.nlm.nih.gov/26223520), licensed under a CC-BY license. Not internally tested by Novus Biologicals.

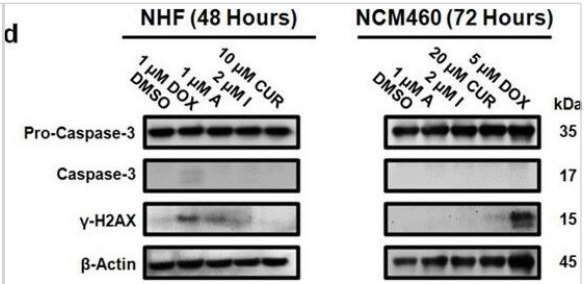

Aβ facilitates HIF1α synthesis and autophagy inhibition via mTOR activation. (A) SK-N-MC cells were exposed to Aβ (5 μM) for 0–48 h. HIF1α and β-actin expression was analyzed by western blot. n = 3. (B) Cells were pretreated with NAC (1 mM) for 30 min prior to Aβ treatment for 24 h. HIF1α and β-actin expression were analyzed by western blot. n = 3. (C,E) Cells were incubated with rapamycin (10 nM) for 30 min prior to Aβ treatment for 24 h. Phosphorylation of 4EBP1 (Thr 37/46) and 4EBP1, phosphorylation of p70S6K1 (Thr 389), HIF1α and β-actin were analyzed by western blot. n = 6. (D) Protein samples were immunoprecipitated by eukaryotic translation initiation factor 4E (eIF4E) antibody-conjugated protein A/G agarose beads. Samples were blotted with 4EBP1 and eIF4E-specific antibodies. n = 3. (F) Cells were exposed to PF4708671 (10 μM) for 30 min prior to Aβ treatment for 24 h. HIF1α and β-actin expression was detected by western blot. n = 6. (G) Cells were exposed to cycloheximide (4 μM) for 30 min prior to Aβ treatment for 24 h. HIF1α and β-actin expressions were detected by western blot. n = 6. (H) Cells were pretreated with rapamycin (10 nM) for 30 min, incubated with Aβ for 24 h and analyzed by western blotting with LC3, p62 and β-actin specific antibodies. n = 3–6. (I) LC3 puncta was visualized by confocal microscopy. Presented results are merged images. Green and red fluorescents indicate LC3 and PI respectively. Scale bars, 50 μm (magnification × 600). (J) Cells were pretreated with trehalose (10 μM) for 30 min prior to Aβ treatment for 24 h. Cytotoxicity was measured by MTT assay at an absorbance of 545 nm using a microplate reader. Data present the mean ± SE. n = 6. (K) Cell viability was measured by trypan blue exclusion assay. Data are presented as a mean ± SE. n = 6. Each blot image was presented as representative image. *p < 0.05 vs. control, #p < 0.05 vs. Aβ treatment. Image collected and cropped by CiteAb from the following open publication (https://pubmed.ncbi.nlm.nih.gov/28790888), licensed under a CC-BY license. Not internally tested by Novus Biologicals.

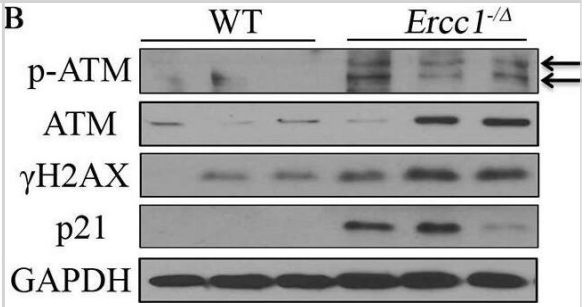

HIF1α drives the expression of PFKFB3 in β-cells. a Luciferase assay showing the activation of PFKFB3 promoter containing 2 hypoxia elements. INS 832/13 overexpressing LacZ or hIAPP were transfected for 36 h with plasmid vectors containing: RenSP luciferase gene without a promoter (empty vector—EV) measuring the background signal or housekeeping gene promoter driving the expression of RenSP luciferase gene (β-actin) or PFKFB3 promoter with hypoxia elements driving the expression of RenSP luciferase gene (PFKFB3). b Representative Western blot of HIF1α, PFKFB3, LDHA, Cdh1 in whole cell extracts of INS 832/13 overexpressing LacZ (CTRL) or hIAPP, silenced or not with short hairpin RNA for PFKFB3 (PFKFB3 shRNA) and HIF1α (HIF1α shRNA) for 36 h. CTRL shRNA is non-target shRNA control vector. β-actin and GAPDH were used as loading control. Data are presented as mean ± SEM, n = 9 independent biological samples (in (a)). Statistical significance was analyzed by unpaired t-test (*p < 0.05) Image collected and cropped by CiteAb from the following open publication (https://pubmed.ncbi.nlm.nih.gov/31213603), licensed under a CC-BY license. Not internally tested by Novus Biologicals.

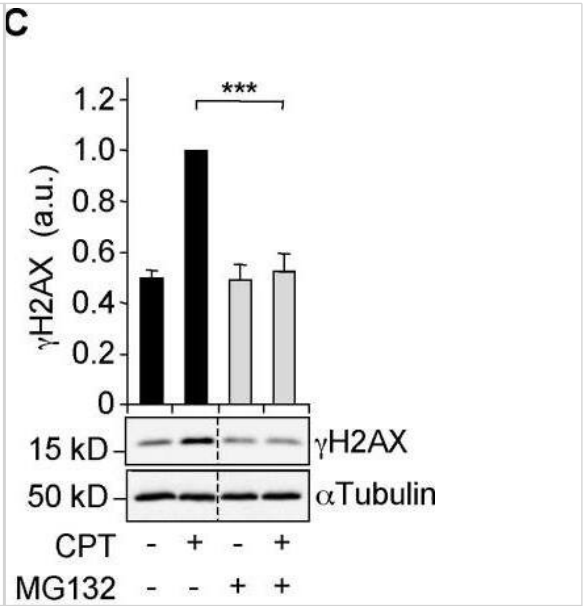

Ddx19 interacts with MKL1 RPEL domain and Ipoβ.(a) Ddx19 recruitment from Hela cell lysate by GST-RPEL and GST-Ipoβ (left). WB, western blotting; (−), without Ran-Q69L; (+), with RanQ69L. Corresponding GST baits are stained with Ponceau to ensure the equal loading of the samples (below). Input sample corresponds to 5% of the Hela cell lysate used in the assay. (b) GST-RPEL was used as a bait for pull down of Ddx19 and Ipoβ from the Hela cell lysate in the presence of increasing amounts of LatB-actin (0.25–10 μM) (left). Arrow indicates the increasing amounts of actin in the corresponding Ponceau staining (below). Image collected and cropped by CiteAb from the following open publication (https://www.nature.com/articles/ncomms6978), licensed under a CC-BY license. Not internally tested by Novus Biologicals.

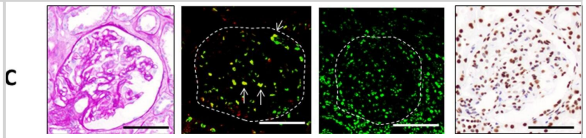

Western blot analysis of co-immunoprecipitations of asynchronous HN30 non-treated and HN30 cells transfected with pcDNA 3.0 NSP 5a3a and pcDNA 3.1/CT-GFP for 3 daysNT: non-treated HN30 cells, TRD: HN30 cells over-expressing NSP 5a3a. a. Immunoprecipitation of non-treated HN30 cells using rabbit anti-NSP 5a3a and western blot analysis using rabbit anti-DAXX., b. Immunoprecipitation of HN30 treated cells using rabbit anti-NSP 5a3a and western blot anaylsis using rabbit anti-DAXX., c. Immunoprecipitation of non-treated HN30 cells using rabbit anti-NSP 5a3a and western blot analysis using rabbit anti-TRAF2., d. Immunoprecipitation of HN30 treated cells using rabbit anti-NSP 5a3a and western blot analysis using rabbit anti-TRAF2., e. Immunoprecipitation of non-treated HN30 cells using rabbit anti-TRAF2/DAXX and western blot analysis using rabbit anti-NSP 5a3a, and f. Immunoprecipitation of HN30 treated cells using rabbit anti-TRAF2/DAXX and western blot analysis using rabbit anti-NSP 5a3a. Image collected and cropped by CiteAb from the following open publication (https://www.oncotarget.com/lookup/doi/10.18632/oncotarget.306), licensed under a CC-BY license. Not internally tested by Novus Biologicals.

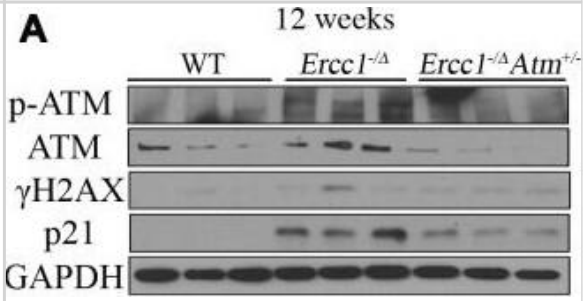

DHA enhances autophagy in MM cells, which contributes to DHA-induced cell deathRPMI-8226 (A) and OPM-2 (B) were cultured with vehicle (Ctrl) or 100 μM DHA for 24 hours in the presence or in the absence of Bafilomycin (Baf) and the expression of the autophagic markers such as LC3I/II and p62 was analyzed by Western blot; β-actin was included as control; numbers indicate band intensities (b.i.) = band volume/area x mean pixel intensity, normalized for β-actin and quantified using Quantity One 1-D analysis software; C. RPMI-8226 cells were cultured for 24 hours with vehicle (Ctrl) or 100 μM DHA in presence or absence of 3-MA (0.3 mM) and their viability assessed by trypan blue exclusion assay (left panel) and cytofluorimetry cell cycle analysis of sub-G1 events, representing apoptotic cells (right panel). Representative experiments out of three. Image collected and cropped by CiteAb from the following open publication (https://www.genesandcancer.com/lookup/doi/10.18632/genesandcancer.131), licensed under a CC-BY license. Not internally tested by Novus Biologicals.

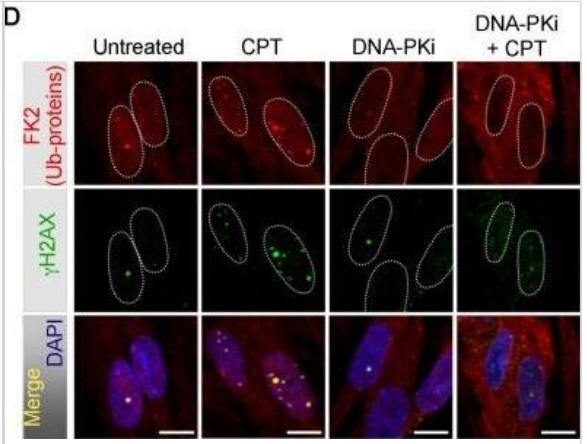

POT1 prevents DDR in human HSC. a Expression of POT1 in hCB CD34+ cells and LT-HSCs (Lin–CD34+CD38−CD45RA−CD90+CD49f+). b hCB-derived LT-HSCs were cultured with MTM-POT1. After 10 days of culture, cells were isolated and re-cultured in methylcellulose medium (200 cells per dish). The number of CFU-C and HPP-CFC (>1.0 mm, >2.0 mm) are shown. Data are expressed as the mean ± SD (n = 3, *p < 0.01 by t-test). Representative data from three independent experiments are shown. c, d hCB LT-HSCs were cultured for 10 days with control MTM protein or MTM-POT1. After 10 days of culture, LT-HSCs were re-isolated and number of TIF was examined. c Immunocytochemical staining of TRF1 (green), 53BP1 (red), and TOTO3 (blue). Scale bar, 2 μm (left). Frequencies of TIFs after 10 days of culture (right). Data are expressed as the mean ± SD (n = 100: control, n = 100: MTM-POT1, *p < 0.01 by t-test). Representative data from 2 independent experiments are shown. d Immunocytochemical staining of TRF1 (green), RPA32 (red), and TOTO3 (blue). Scale bar, 2 μm (left). Frequencies of TIFs after 10 days of culture (right). Data are expressed as the mean ± SD (n = 110–120: control, n = 110: MTM-POT1, *p < 0.01 by t-test). Representative data from two independent experiments are shown Image collected and cropped by CiteAb from the following open publication (https://pubmed.ncbi.nlm.nih.gov/28986560), licensed under a CC-BY license. Not internally tested by Novus Biologicals.

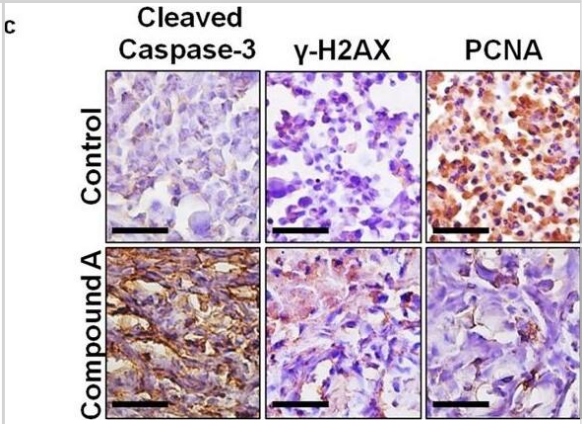

Cell numbers positively stained for NeuN, DCX, PCNA and caspase-3 in the subgranular region of the dentate gyrus in WT and RanBP9−/− (KO) mice.(A), DAPI-stained brain sections to show the highlighted subgranular zone within the dentate gyrus region of the hippocampus used for cell counts shown in B. (B), Representative brain sections stained with anti-NeuN, anti-DCX, anti-PCNA, anti-capsase-3 and counter stained with DAPI. Cell counting revealed significantly decreased numbers of NeuN positive cells in RanBP9−/− (KO) brains (22%) compared to WT controls. However DCX, PCNA and caspase positive cell numbers were not significantly altered. In each group, n=3, data presented as mean± SEM. **, p<0.01 by Student's t-test. Image collected and cropped by CiteAb from the following open publication (https://pubmed.ncbi.nlm.nih.gov/23840553), licensed under a CC-BY license. Not internally tested by Novus Biologicals.

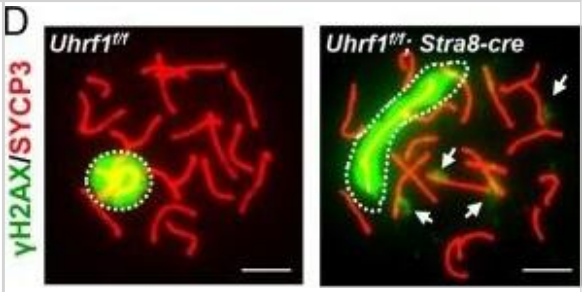

SAN1 functions independently of the FA pathway and does not affect FA pathway activation. a, b CSAs of HeLa WT and SAN1−/− cells treated with scrambled ctrl siRNA or FANCD2 siRNA, in response to Cisplatin and MMC (N = 3). Statistical significance determined by two-way ANOVA. Error bars denote s.e.m. *p < 0.05, **p < 0.01, ***p < 0.001, ****p < 0.0001. c Immunoblot showing siRNA knockdown of FANCD2 in HeLa WT and SAN1−/− cells. d IF staining of FANCD2 foci in HeLa WT cells and SAN1−/− cells treated with 0.045 μM MMC. e Immunoblot of FANCD2 showing mono-ubiquitylation in HeLa WT and SAN1−/− cells treated with vehicle or 0.045 μM MMC. f, g CSAs of HeLa WT and SAN1−/− cells treated with ctrl or SNM1A siRNA and exposed to Cisplatin or MMC. Statistical significance was determined by two-way ANOVA test. h Immunoblot of SNM1A in HeLa WT and SAN1−/− cells treated with ctrl or SNM1A siRNA Image collected and cropped by CiteAb from the following open publication (https://pubmed.ncbi.nlm.nih.gov/29968717), licensed under a CC-BY license. Not internally tested by Novus Biologicals.

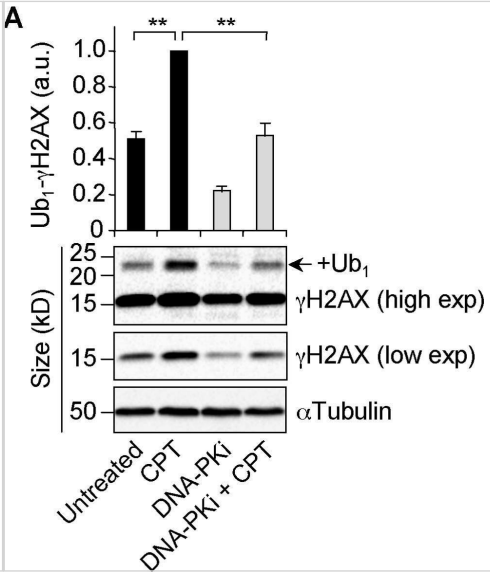

Publications

Audet-Delage Y, St-Louis C, Minarrieta L et al. Spatiotemporal modeling of chemoresistance evolution in breast tumors uncovers dependencies on SLC38A7 and SLC46A1 Cell reports 2023-10-31 [PMID: 37792528] (FLOW, Human)

Wu D, Huang H, Chen T et al. The BRCA1/BARD1 complex recognizes pre-ribosomal RNA to facilitate homologous recombination Cell discovery 2023-10-03 [PMID: 37789001]

Ershova ES, Savinova EA, Kameneva LV et al. Satellite III (1q12) Copy Number Variation in Cultured Human Skin Fibroblasts from Schizophrenic Patients and Healthy Controls Frontiers in bioscience (Landmark edition) 2023-08-31 [PMID: 37664948] (FLOW, Human)

McCann JL, Cristini A, Law EK et al. APOBEC3B regulates R-loops and promotes transcription-associated mutagenesis in cancer Nature genetics 2023-09-21 [PMID: 37735199] (ICC/IF, Human)

Hishikawa A, Hayashi K, Kubo A et al. DNA repair factor KAT5 prevents ischemic acute kidney injury through glomerular filtration regulation iScience 2021-12-17 [PMID: 34877495]

Herok M, Wawrzynow B, Maluszek MJ et al. Chemotherapy of HER2- and MDM2-Enriched Breast Cancer Subtypes Induces Homologous Recombination DNA Repair and Chemoresistance Cancers (Basel) 2021-09-07 [PMID: 34572735]

Fielder E, Wan T, Alimohammadiha G et al. Short senolytic or senostatic interventions rescue progression of radiation-induced frailty and premature ageing in mice eLife 2022-05-04 [PMID: 35507395]

Pai G, Roohollahi K, Rockx D et al. Genome-wide siRNA screens identify RBBP9 function as a potential target in Fanconi anaemia-deficient head-and-neck squamous cell carcinoma Communications Biology 2023-01-13 [PMID: 36639418] (WB)

Hindle A, Koneru B, Makena MR et al. The O6-methyguanine-DNA methyltransferase inhibitor O6-benzylguanine enhanced activity of temozolomide + irinotecan against models of high-risk neuroblastoma Anti-Cancer Drugs 2021-03-01 [PMID: 33323683] (WB, B/N)

□oku J, Booth DM, Skoda J et al. Reduced ER-mitochondria connectivity promotes neuroblastoma multidrug resistance The EMBO Journal 2022-04-19 [PMID: 35211994]

Nonaka K, Takubo K, Aida J et al. Accelerated telomere shortening in adrenal zona reticularis in patients with prolonged critical illness Front Endocrinol (Lausanne) 2023-09-04 [PMID: 37745694] (IHC)

Sakama S, Kurusu K, Morita M et al. An Enriched Environment Alters DNA Repair and Inflammatory Responses After Radiation Exposure Frontiers in Immunology 2021-10-22 [PMID: 34745135]

More publications at http://www.novusbio.com/NB100-384

Novus Biologicals USA
10730 E. Briarwood Avenue
Centennial, CO 80112
USA
Phone: 303.730.1950
Toll Free: 1.888.506.6887
Fax: 303.730.1966
nb-customerservice@bio-techne.com

Bio-Techne Canada
21 Canmotor Ave
Toronto, ON M8Z 4E6
Canada
Phone: 905.827.6400
Toll Free: 855.668.8722
Fax: 905.827.6402
canada.inquires@bio-techne.com

Bio-Techne Ltd
19 Barton Lane
Abingdon Science Park
Abingdon, OX14 3NB, United Kingdom
Phone: (44) (0) 1235 529449
Free Phone: 0800 37 34 15
Fax: (44) (0) 1235 533420
info.EMEA@bio-techne.com

General Contact Information
www.novusbio.com
Technical Support: nb-technical@bio-techne.com
Orders: nb-customerservice@bio-techne.com
General: novus@novusbio.com

Products Related to NB100-384

NBL1-11424	Histone H2AX Overexpression Lysate
HAF008	Goat anti-Rabbit IgG Secondary Antibody [HRP]
NB7160	Goat anti-Rabbit IgG (H+L) Secondary Antibody [HRP]
NBP2-24891	Rabbit IgG Isotype Control

Limitations

This product is for research use only and is not approved for use in humans or in clinical diagnosis. Primary Antibodies are guaranteed for 1 year from date of receipt.

For more information on our 100% guarantee, please visit www.novusbio.com/guarantee

Earn gift cards/discounts by submitting a review: www.novusbio.com/reviews/submit/NB100-384

Earn gift cards/discounts by submitting a publication using this product: www.novusbio.com/publications